© 2018. Published by The Company of Biologists Ltd | Journal of Experimental Biology (2018) 221, jeb173948. doi:10.1242/jeb.173948

RESEARCH ARTICLE

Renoguanylin stimulates apical CFTR translocation and decreases HCO_3^- secretion through PKA activity in the Gulf toadfish (*Opsanus beta*)

Ilan M. Ruhr[1,*,‡], Kevin L. Schauer[1], Yoshio Takei[2] and Martin Grosell[1]

ABSTRACT

The guanylin peptides – guanylin, uroguanylin and renoguanylin (RGN) – are endogenously produced hormones in teleost fish enterocytes that are activators of guanylyl cyclase-C (GC-C) and are potent modulators of intestinal physiology, particularly in seawater teleosts. Most notably, they reverse normal net ion-absorbing mechanisms that are vital to water absorption, an important process for seawater teleost survival. The role of guanylin-peptide stimulation of the intestine remains unclear, but it is hypothesized to facilitate the removal of solids from the intestine by providing fluid to enable their removal by peristalsis. The present study used one member of this group of peptides – RGN – to provide evidence for the prominent role that protein kinase A (PKA) plays in mediating the effects of guanylin-peptide stimulation in the posterior intestine of the Gulf toadfish (*Opsanus beta*). Protein kinase G was found to not mediate the intracellular effects of RGN, despite previous evidence showing that GC-C activation leads to higher cyclic guanosine monophosphate formation. RGN reversed the absorptive short-circuit current and increased conductance in the Gulf toadfish intestine. These effects are correlated to increased trafficking of the cystic fibrosis transmembrane conductance regulator (CFTR) Cl^- channel to the apical membrane, which is negated by PKA inhibition. Moreover, RGN decreased HCO_3^- secretion, likely by limiting apical HCO_3^-/Cl^- exchange (possibly by reducing SLC26a6 activity), a reduction that was enhanced by PKA inhibition. RGN seems to alter PKA activity in the posterior intestine to recruit CFTR to the apical membrane and reduce HCO_3^- secretion.

KEY WORDS: PKG, Cl^- secretion, Guanylin peptides, Intestine, Seawater teleost

INTRODUCTION

Seawater presents a major osmoregulatory challenge for teleost fish, because of the direct interaction of their thin respiratory epithelia – the gills – with the environment, which causes unavoidable branchial fluid loss (Evans et al., 2005). To compensate, the seawater teleost constantly drinks water and absorbs it across the intestine. Imbibed seawater undergoes rapid desalination by the esophagus, so, by the time it enters the intestine, its osmolality is roughly that of blood plasma. In the intestine, precipitation of Ca^{2+} and Mg^{2+} by HCO_3^- to form $CaCO_3$ and $MgCO_3$ precipitates and titration of HCO_3^- by H^+ facilitate further decreases in intestinal fluid osmolality by up 130 mOsmol kg^{-1} (Grosell et al., 2009a,b; Wilson et al., 2002). The combined effect of these processes, in addition to other ion-absorbing pathways, renders the fluid osmolality in the intestine similar to that of the extracellular fluids and allows for efficient water absorption that is coupled to Na^+ and Cl^- absorption (Skadhauge, 1969, 1974). Even though net water absorption and the mechanisms that facilitate it are vital to the survival of teleosts living in seawater, recent studies reveal region-specific areas of the intestine that display net secretory functions, at least periodically (Ruhr et al., 2014, 2016).

In the Gulf toadfish, *Opsanus beta* (Goode and Bean, 1880), members of the homologous guanylin family of intestinal peptides [guanylin, uroguanylin and renoguanylin (RGN)] reverse ion absorption in the posterior intestine, but not in the anterior region (Ruhr et al., 2014). This reversal also corresponds to RGN-stimulated water secretion in the posterior intestine and rectum, but not in the anterior intestine (Ruhr et al., 2014, 2016). The switch from net ion absorption to net ion secretion (from mucosa-to-serosa to serosa-to-mucosa) seems to be caused primarily by inhibiting ion absorption by the $Na^+/K^+/Cl^-$-cotransporter type 2 (NKCC2) and limiting HCO_3^-/Cl^- exchange activity, as well as activating Cl^- secretion through the apical cystic fibrosis transmembrane conductance regulator (CFTR) channel (Ruhr et al., 2014, 2015, 2016). This response is also isolated to the mid and posterior intestine of the Japanese eel (*Anguilla japonica*) after stimulation by guanylin (Ando and Takei, 2015; Ando et al., 2014; Yuge and Takei, 2007). It is hypothesized that the inhibition of fluid absorption is required to facilitate the removal of solids, such as undigested food, fecal matter or carbonate precipitates. The presence of fluid has been shown to enhance the efficiency of peristalsis in mammals, thus making the movement of solids through the intestinal tract easier (Schulze, 2015).

A handful of studies on the intestinal physiology of seawater teleosts have demonstrated a reversal of ion absorption. In the winter flounder (*Pseudopleuronectes americanus*) intestine, atrial natriuretic factor, vasoactive intestinal peptide (VIP), cyclic guanosine monophosphate (cGMP) and cyclic adenosine monophosphate (cAMP) can alter NKCC2 activity and decrease the absorptive short-circuit current (I_{SC}), which is a measure of total ion movement (O'Grady, 1989; O'Grady et al., 1988, 1985; Rao and Nash, 1988; Rao et al., 1984). These early studies demonstrated that the reversal of net ion absorption in seawater teleosts is largely driven by Cl^- secretion, in addition to decreased activity of absorptive-type ion transporters (O'Grady and Wolters, 1990). A

[1]Department of Marine Biology and Ecology, The Rosenstiel School of Marine and Atmospheric Science, The University of Miami, Miami, FL 33149, USA. [2]Department of Marine Bioscience, The Atmosphere and Ocean Research Institute, The University of Tokyo, Kashiwa, Chiba, Japan.
*Present address: Faculty of Biology, Medicine and Health, University of Manchester, Core Technology Facility, 46 Grafton Street, Manchester M13 9NT, UK.

‡Author for correspondence (ilan.ruhr@manchester.ac.uk)

I.M.R., 0000-0001-9243-7055; K.L.S., 0000-0002-3677-250X; Y.T., 0000-0003-3004-8905

Received 7 November 2017; Accepted 15 January 2018

Journal of Experimental Biology (2018) 221, jeb173948. doi:10.1242/jeb.173948

List of symbols and abbreviations

cAMP	cyclic adenosine monophosphate
CFTR	cystic fibrosis transmembrane conductance regulator
cGMP	cyclic guanosine monophosphate
GC-C	guanylyl cyclase-C
G_{TE}	transepithelial conductance
H-89	PKA inhibitor
I_{SC}	short-circuit current
KT5823	PKG inhibitor
NHE	Na^+/H^+ exchanger
NKCC2	$Na^+/K^+/2Cl^-$ symporter
PKA	protein kinase A
PKG	protein kinase G
PKI	PKA inhibitor
RGN	renoguanylin
SLC26a6	solute carrier family 26 member 6 (HCO_3^-/Cl^--antiporter)
TEP	transepithelial potential
VIP	vasoactive intestinal peptide

more recent study on the killifish (*Fundulus heteroclitus*) similarly revealed that a combination of ionomycin, dibutyryl-cAMP and IBMX (a phosphodiesterase inhibitor) stimulates fluid secretion in the posterior intestine (Marshall et al., 2002). It is interesting that intestinal tissues from multiple species of seawater teleosts respond to the above-mentioned hormones, activators and inhibitors by decreasing ion-absorbing mechanisms that, in some cases, result in fluid secretion. The inhibition of ion transport and water absorption is widespread across seawater teleost species and might serve a beneficial purpose for life in seawater. In both mammalian and fish enterocytes, stimulation of the apical guanylin peptide receptor guanylyl cyclase-C (GC-C) leads to increased formation of cGMP (Chao et al., 1994; Kuhn et al., 1994; Schulz et al., 1990; Yuge and Takei, 2007), which activates protein kinase G (PKG) and increases cAMP formation [leading to protein kinase A (PKA) activation] (Arshad and Visweswariah, 2012, 2013). Stimulation of GC-C leads to apical CFTR activation, inhibition of Na^+/H^+-exchangers (NHEs) in mammals, inhibition of NKCC2 in fish and a decrease in HCO_3^- secretion in fish (Chao et al., 1994; Ruhr et al., 2014, 2016).

In the present study, we investigated the intracellular effects of RGN in Gulf toadfish enterocytes. Our first goal was to determine whether RGN affected CFTR abundance in the apical membrane. We have previously shown that CFTR is likely present in the posterior intestine of the Gulf toadfish, but that it is mostly sub-apical. We hypothesize that RGN stimulation will increase insertion of CFTR into the apical membrane. The present study corroborates these findings by measuring the I_{SC} and transepithelial conductance (G_{TE}) of the tissues. Our second goal was to see whether the RGN response was mediated primarily by PKG or PKA. We hypothesize that PKA plays a greater role in mediating the RGN response, based partly on the fact that cAMP/PKA is involved in trafficking CFTR in the rat jejunum and in *Xenopus laevis* oocytes (Golin-Bisello et al., 2005; Weber et al., 1999).

Table 1. Composition of salines for short-circuit current, pH-stat titration and sac preparation experiments

Compound	Mucosal*	Serosal	HCO_3^-/CO_2-free serosal
NaCl (mmol l^{-1})	169.0	151.0	151.0
KCl (mmol l^{-1})	5.0	3.0	3.0
$MgSO_4$ (mmol l^{-1})	77.5	0.88	0.88
$MgCl_2$ (mmol l^{-1})	22.5		
Na_2HPO_4 (mmol l^{-1})		0.5	0.5
KH_2PO_4 (mmol l^{-1})		0.5	0.5
$CaCl_2$ (mmol l^{-1})	5.0	1.0	1.0
$NaHCO_3$ (mmol l^{-1})		5.0	
Hepes, free acid (mmol l^{-1})		11.0	11.0
Hepes, Na^+ salt (mmol l^{-1})		11.0	11.0
Urea (mmol l^{-1})		4.5	4.5
Glucose (mmol l^{-1})		5.0	5.0
Osmolality (mosmol kg^{-1} H_2O)§	330	330	330
pH	7.8¶	7.8	7.8
Gas‡	100% O_2	0.3% CO_2 in O_2	100% O_2

*Activators and inhibitors (in final concentrations) were applied to the mucosal saline: renoguanylin (0.1 and 0.5 μmol l^{-1}), KT5823 (2 μmol l^{-1}), Rp-8-pCPT-cGMPS (25 μmol l^{-1}), 8-bromo-cGMP (100 μmol l^{-1}), H-89 (20 μmol l^{-1}) and PKI (10 μmol l^{-1}). §The osmolality of salines was adjusted with mannitol. ¶When measuring HCO_3^- secretion, mucosal pH in Ussing chambers was maintained at 7.8 by pH-stat titration. ‡Salines were gassed for at least 1 h prior to experiments.

MATERIALS AND METHODS

Experimental animals

Gulf toadfish were caught as bycatch from Biscayne Bay, FL, USA. Upon arrival in the laboratory, ectoparasites were removed by a 3 min freshwater bath and treatment with Malachite Green in seawater. Fish were separated by size/mass classes and placed into 62 l aerated tanks (33–36 ppt, 20–26°C), with continuous flow-through of sand-filtered seawater from Biscayne Bay. Fish were fed weekly to satiation with squid, but fasted for at least 3 days prior to experimentation. Fish husbandry and experimental procedures were in accordance with the University of Miami Animal Care Protocol (IACUC no. 13-225, renewal 03, and 15-019, renewal 02). MS-222 (0.2 g l^{-1}; Argent, Redmond, WA, USA) solution, buffered with 0.3 g l^{-1} $NaHCO_3^-$ (Sigma-Aldrich, St Louis, MO, USA), was used to anesthetize fish; they were then killed by severing the spinal cord at the cervical vertebra and pithing of the brain.

Composition of salines, hormones, activators and inhibitors

Mucosal (pH 7.8) and serosal (pH 7.8) salines were prepared as described in Table 1 and used to bathe intestinal tissues. Eel RGN (Peptide Institute, Ibaraki-Shi, Osaka, Japan) was used in the present study as the activator and a tool to assess the function of activating GC-C in the posterior intestine. The purity of biologically active eel RGN was confirmed using reversed-phase, high-performance liquid chromatography (Yuge and Takei, 2007). The amino acid sequence of eel RGN (ADLCEICAFAACTGCL, accession number: BAC76010.1) is nearly identical to that of Gulf toadfish guanylin (MDVCEICAFAACTGC, accession number: AIA09902.1) and stimulation of the Gulf toadfish posterior intestine with eel RGN has the greatest physiological effects compared with those of eel uroguanylin or eel guanylin (Ruhr et al., 2014).

Activators and inhibitors were dissolved in water, dimethylsulfoxide (DMSO; Sigma-Aldrich) or ethanol (EtOH; Sigma-Aldrich). The PKG inhibitors KT5823 and Rp-8-pCPT-cGMPS (Enzo Life Sciences, Farmingdale, NY, USA) were dissolved in DMSO and water, respectively. The cGMP analog/PKG activator 8-bromo-cGMP (Enzo) was dissolved in water. The PKA inhibitors H-89 (dihydrochloride; Cell Signaling Technologies, Beverly, MA, USA) and protein kinase inhibitor (PKI) (14-22, amide, myristoylated; Enzo) were dissolved in DMSO. Final concentrations were as follows: KT5823, 2 μmol l^{-1}; Rp-8-pCPT-cGMPS, 25 μmol l^{-1}; 8-bromo-cGMP, 100 μmol l^{-1}; H-89, 20 μmol l^{-1}; and PKI, 10 μmol l^{-1}. The concentrations for

Journal of Experimental Biology (2018) 221, jeb173948. doi:10.1242/jeb.173948

these inhibitors were tested using the dose recommended by their respective manufacturers (and not surpassing the solubility that would exceed the ideal DMSO or EtOH content in the saline). Final solvent ratios in which inhibitors were dissolved were 1:1000 (0.1%) and 1:2000 (0.05%) for DMSO and EtOH, respectively. Vehicle controls for 0.1% DMSO and 0.05% EtOH did not affect the physiological parameters tested in the present (data not shown) and previous studies on Gulf toadfish (Ruhr et al., 2014, 2015, 2016).

General experimental protocol: I_{SC} and pH-stat titration

I_{SC}, transepithelial potential (TEP) and G_{TE} of Gulf toadfish tissues were measured by Ussing chambers (model 2400; Physiologic Instruments, San Diego, CA, USA). The posterior intestine of a Gulf toadfish (15–30 g) was excised, cut open along the midline, mounted onto P2413 tissue holders (Physiologic Instruments) to expose 0.71 cm^2 of tissue, and placed between the two half-chambers of the Ussing apparatus. I_{SC} and TEP were measured by silver (Ag) current and Ag/AgCl voltage electrodes, respectively, and were connected to an amplifier (model VCC600, Physiologic Instruments). I_{SC} was measured using current electrodes under voltage-clamp conditions (0 mV), with 3 s of 2 mV pulses (mucosal-to-serosal) every 60 s. TEP was measured by voltage electrodes under current-clamp conditions (0 µA), with 3 s of 30 µA pulses (mucosal-to-serosal) every 60 s. G_{TE} was calculated by Ohm's law and was determined from the deflections in I_{SC} and TEP during pulsing. Acqknowledge software (v.3.8.1, BIOPAC Systems, Goleta, CA, USA) recorded I_{SC} and TEP onto a computer. The function and viability of Gulf toadfish intestinal tissues are stable in the Ussing chamber for more than 2 h (Ruhr et al., 2014).

I_{SC} measurements were taken under symmetrical conditions using 2 ml of serosal saline (Table 1) in each half-chamber (the mucosal/apical/luminal and the serosal/basolateral/blood-side chambers). The salines were continually mixed by airlift gassing (0.3% CO_2/99.7% O_2) and maintained at 25°C by a recirculating bath (model 1160S, VWR, Radnor, PA, USA), as described in Grosell and Genz (2006).

TEP measurements were taken under asymmetrical conditions using 2 ml each of mucosal and HCO_3^-/CO_2-free serosal saline (Table 1), which were added to their respective half-chambers. A previous study on the Gulf toadfish revealed that RGN might regulate the transport activity of apical HCO_3^- transporters, such as SLC26a6 (Ruhr et al., 2016). This previous study used an HCO_3^-/CO_2-free serosal saline to render the basolateral NBCe (an electrogenic Na^+/HCO_3^--cotransporter) functionless and determined that the effects of RGN decreased apical HCO_3^- secretion, independent of cytosolic carbonic anhydrase activity. Accordingly, the present study also used a HCO_3^-/CO_2-free serosal saline to investigate the role of PKA and PKG activators and inhibitors on apical HCO_3^- transport activity. The mucosal and serosal saline were continually mixed by airlift gassing (100% O_2) as described above and maintained at 25°C. HCO_3^- secretion was measured using a pH-stat titrator (model TIM 854 or 856, Radiometer, Loveland, CO, USA) that was set up in tandem with an Ussing chamber system (described by Grosell and Genz, 2006). A mucosal pH of 7.8 was maintained using a pH electrode (Radiometer, model PHC4000.8) and an acid-delivering microburette tip (0.005 mol l^{-1} HCl); both were immersed in the mucosal saline bath, allowing for symmetrical pH conditions on either side of the epithelium. The volume of acid titrant and mucosal pH was measured and recorded onto a computer using Titramaster software (Radiometer, v.5.1.0). The HCO_3^- secretion rate from a tissue preparation was calculated from the rate of titrant secreted and its concentration (described by Grosell and Genz, 2006). RGN was added to the mucosal half-chamber, to a concentration of 0.1 µmol l^{-1}.

Table 2. *P*-values for the results of two-tailed Holm–Sidak tests used in the present study

Corresponding figure	Variable	Comparison	*P*-value
2A	I_{sc}	RGN vs control	<0.001
		KT5823 vs control	<0.001
2B	G_{TE}	RGN vs control	<0.001
		KT5823 vs control	<0.001
3A	I_{sc}	RGN vs control	<0.001
		RGN+H-89 vs control	<0.001
		RGN vs RGN+H-89	0.01
3B	G_{TE}	RGN vs control	0.003
		RGN+H-89 vs control	0.05
		RGN vs RGN+H-89	0.065
3C	I_{sc}	H-89 vs control	<0.001
		H-89+RGN vs control	<0.001
		H-89 vs H-89 RGN	0.001
3D	G_{TE}	H-89 vs control	<0.001
		H-89+RGN vs control	0.023
		H-89 vs H-89+RGN	<0.001
4B	Band intensity	RGN vs control	0.024
6A	HCO_3^- secretion	RGN vs control	0.034
		RGN+H-89 vs control	0.002
		RGN vs RGN+H-89	0.032
6B	TEP	RGN vs control	0.008
		RGN+H-89 vs control	0.019
		RGN vs RGN+H-89	0.031
6B	G_{TE}	RGN vs control	0.171
		RGN+H-89 vs control	0.011
		RGN vs RGN+H-89	0.002
6C	HCO_3^- secretion	H-89 vs control	0.300
		H-89+RGN vs control	0.159
		H-89 vs H-89 RGN	0.043
6D	TEP	H-89 vs control	0.002
		H-89+RGN vs control	<0.001
		H-89 vs H-89 RGN	0.232
6D	G_{TE}	H-89 vs control	0.255
		H-89+RGN vs control	0.018
		H-89 vs H-89 RGN	0.004

I_{SC}, short-circuit current; G_{TE}, transepithelial conductance; TEP, transepithelial potential.

Intestinal sac preparations and immunohistochemistry

Sac preparations from the posterior intestine were made and preserved for immunohistochemistry to determine the effects of RGN on CFTR translocation. The posterior intestine (1.5–3 cm) from Gulf toadfish (50–80 g) was excised as described above. Briefly, following a modified protocol (Ruhr et al., 2016), the flared end of a PE50 catheter was inserted into the posterior intestine and tied off with a silk suture. Mucosal saline (Table 1) was then injected into the catheter to rinse the tissue of any debris. The open end of the tissue was then tied off with a silk suture to form an intestinal sac.

Journal of Experimental Biology (2018) 221, jeb173948. doi:10.1242/jeb.173948

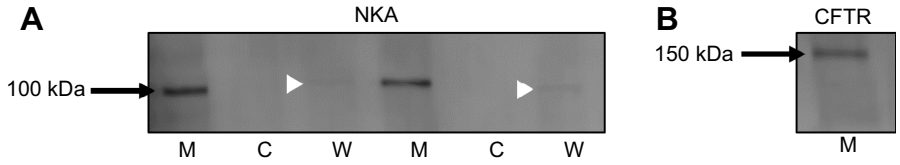

Fig. 1. Membrane protein isolation. Western blots (n=3) for isolated fractions of the posterior intestine from Gulf toadfish reveal specific banding for Na^+/K^+-ATPase (NKA) (A) and cystic fibrosis transmembrane conductance regulator (CFTR) (B). NKA was highly enriched in the membrane fraction (M), and much less so in whole-cell fraction (W), while it was undetectable in the cytoplasmic fraction (C).

The sac preparations were then injected with mucosal saline (control or containing 0.5 µmol l^{-1} RGN). The catheter was sealed and placed in a scintillation vial containing serosal saline and continually gassed with 0.3% CO_2 (Table 1) for 1 h. At the end of the experimental period, the sac preparations were removed from the serosal saline. After the silk sutures were cut and the catheter removed, the tissue was drained and placed in Z-fix (Anatech, Hayward, CA, USA) for 48 h to fix the tissue. Following fixation, the tissue was immersed in 70% ethanol for 1 week. Then, ascending grades of ethanol washes (3 times in 95%, followed by 3 times in 100%) were used to dehydrate tissues. Tissues were then prepared for wax embedding by immersion in butanol, two washes in Histochoice (Amresco, Solon, OH, USA) and four washes in Paraplast Embedding Media (McCormick Scientific, St Louis, MO, USA), after which tissues were embedded in tissue holders containing Paraplast. A microtome (model 1512, Leitz, Grand Rapids, MI, USA) was used to slice sections of tissue (4 µm); the tissue sections from the posterior intestine were mounted onto poly-L-lysine-coated slides and dried for 24 h at 37°C.

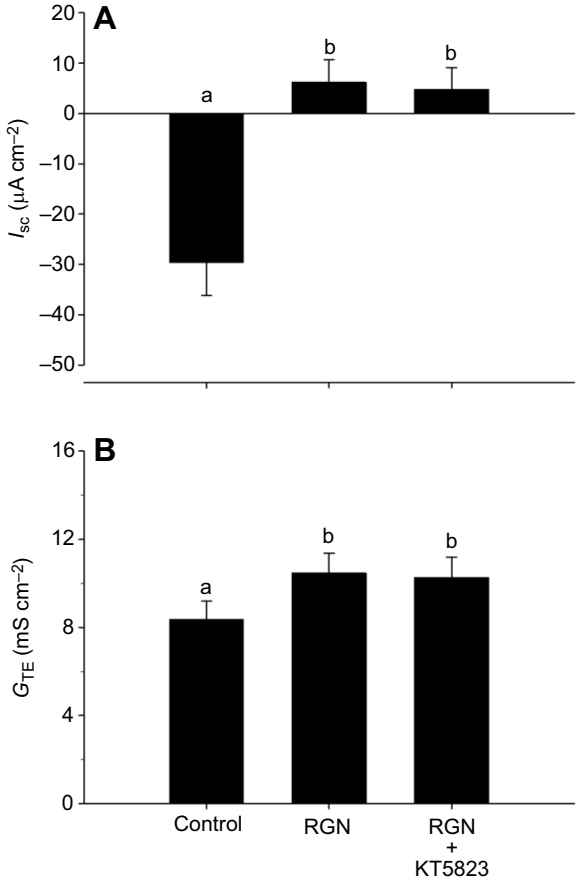

Fig. 2. Modulation of electrophysiology in the posterior intestine. Short-circuit current (I_{SC}) (A) and transepithelial conductance (G_{TE}) (B) displayed by the posterior intestine of Gulf toadfish before and after treatment with renoguanylin (RGN) and combined treatment with RGN and KT5823 [a protein kinase G (PKG) inhibitor]. Pre-treatment values are taken from the final 30 min of the control flux and post-treatment values are taken from the final 30 min of a 70 min treatment flux. Values are means±s.e.m. (n=8). Significant differences were revealed by one-way, repeated-measures ANOVA, followed by one-tailed Holm–Sidak tests ($^{a,b}P \leq 0.05$). Positive and negative I_{SC} values indicate secretory and absorptive currents, respectively. RGN (0.1 µmol l^{-1}, dissolved in H_2O) and KT5823 (2 µmol l^{-1}, dissolved in ethanol, final v/v 0.05%) were added to the mucosal half-chamber of the Ussing apparatus.

Tissues were prepared for antibody treatment by washing slides twice in Histochoice (to remove the paraplast), followed by immersion in descending grades of ethanol (100%, 2×90%, 70% and 50%) and two washes in phosphate-buffered saline (PBS) (pH 7.3). To reveal antigenic sites, the following steps were taken. Slides were first incubated in 10 mmol l^{-1} of citric acid solution (pH 6) and heated to boiling in a microwave (two 5-min incubations at 80% power). Next, slides were cooled to room temperature and were washed in the following order: 0.05% SDS-PBS for 5 min, solution A [PBS, NaCl (58.44 mmol l^{-1}), 0.2% Tween-20 (Sigma-Aldrich) and pH 7.3] for 5 min, and Image-iT (Life Technologies, Carlsbad, CA, USA) for 30 min. To block non-specific antigenic sites, slides were incubated for 1 h in PBS solution containing 5% skimmed milk, 1% bovine serum albumin (BSA), and 0.05% Tween-20. Slides were rinsed twice in PBS after each step.

Tissue sections from the posterior intestine were probed with fluorescent antibodies. The primary monoclonal mouse CFTR antibody [Human CFTR C-Terminus MAb (Clone 24-1), Mouse IgG2A, cat. no. MAB25031, R&D Systems, Minneapolis, MN, USA] was diluted to 10 µg ml^{-1} in PBS solution containing 0.5% skimmed milk, 1% BSA and 0.05% Tween-20. This particular CFTR antibody was used previously by our group to reveal CFTR localization in the intestine of the Gulf toadfish (Ruhr et al., 2014) and has been validated using western blot analysis of CFTR in the Gulf toadfish gill, with an approximate mass of 135 kDa (Zongli Yao, K.L.S., I.M.R., Edward M. Mager, Rachael M. Heuer and M.G., unpublished data). A hydrophobic pen was used to create a border around the tissues on a slide, inside of which primary antibody was deposited. Slides were placed in a humid chamber on an oscillating table at 5°C overnight, then rinsed twice in PBS containing 0.05% Tween-20 and once in normal PBS. The following steps were carried out in the absence of light. Donkey anti-mouse IgG secondary antibody (Alexa Fluor 488, cat. no. AB_2556542, Thermo Fisher Scientific, Waltham, MA, USA) was diluted to 10 µg ml^{-1} in PBS solution containing 0.5% skimmed milk, 1% BSA and 0.05% Tween-20. The anti-mouse IgG was deposited inside the hydrophobic border surrounding the tissues. Slides were incubated in a humid chamber for 1 h at 37°C, after which they were rinsed twice in PBS containing 0.05% Tween-20 and once in normal PBS. ProLong Gold Antifade Reagent (Thermo Fisher Scientific) was used to adhere coverslips onto each slide. Control slides were treated the same as above, with the exception of

Journal of Experimental Biology (2018) 221, jeb173948. doi:10.1242/jeb.173948

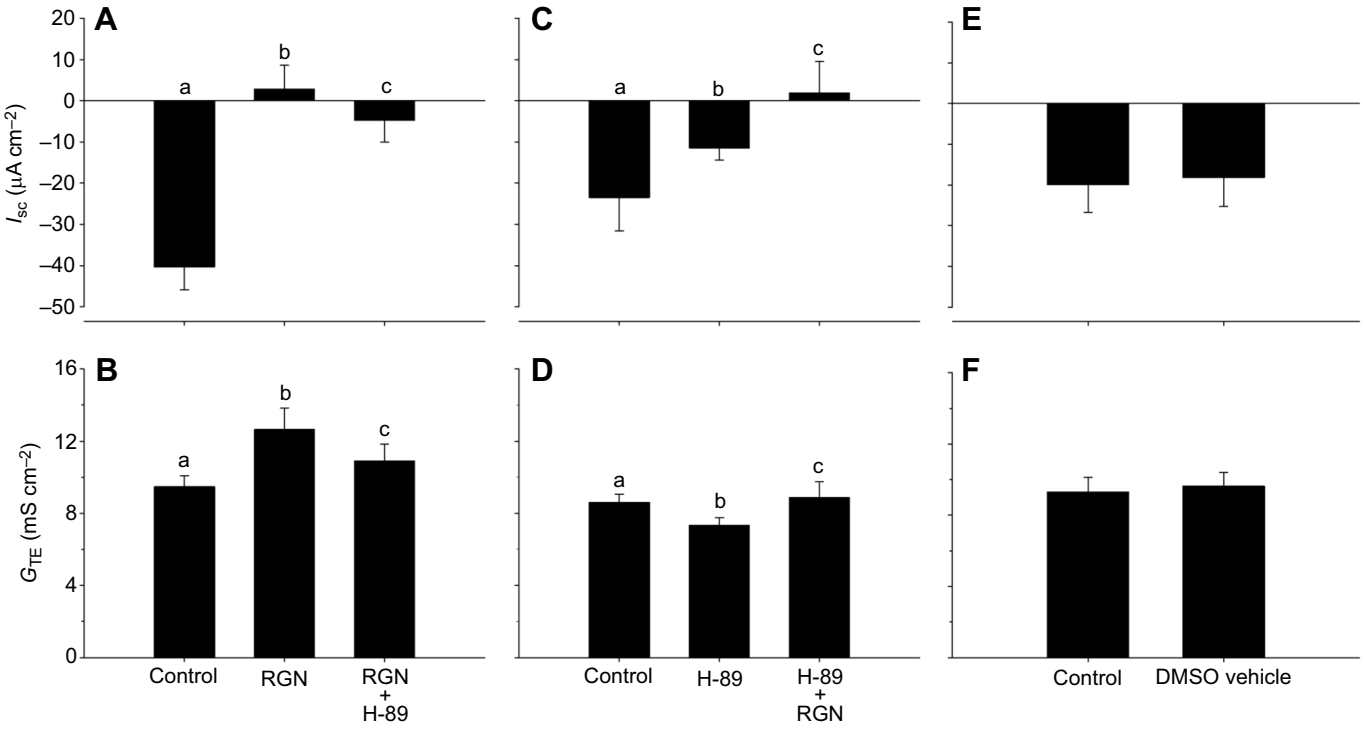

Fig. 3. Modulation of electrophysiology in the posterior intestine. I_{SC} (A,C) and G_{TE} (B,D) displayed by the posterior intestine of Gulf toadfish. The first experiment (A,B) looked at the effects of RGN alone, followed by the addition of H-89 [a protein kinase A (PKA) inhibitor]. The second experiment (C,D) looked at the effects of H-89 alone, followed by the addition of RGN. Dimethyl sulfoxide (DMSO) vehicle, in which H-89 stocks were prepared, had no effect on I_{SC} and G_{TE} (E,F). Pre-treatment values are taken from the final 30 min of the control flux and post-treatment values (including DMSO) are taken from the final 30 min of a 70 min treatment flux. Values are means±s.e.m. (n=6 for all experiments). Significant differences were revealed by one-way, repeated-measures ANOVA, followed by one-tailed Holm–Sidak tests ($^{a,b,c}P \leq 0.05$). Positive and negative I_{SC} values indicate secretory and absorptive currents, respectively. RGN (0.1 μmol l^{-1}, dissolved in H_2O) and H-89 (20 μmol l^{-1}, dissolved in DMSO, final v/v 0.1%) were added to the mucosal half-chamber of the Ussing apparatus.

primary antibody treatment. Slides were observed with an Olympus fluorescence microscope (u-tvo.5xc-2), and images were taken with an attached QImaging camera (Retiga EXi, Fast 1394) using 40× and 60× magnification. Fiji (Schindelin et al., 2012), iVision and Gimp software were used to analyze the images. Three slides were analyzed for each individual (n=4 per treatment).

A modified procedure was used to determine corrected membrane fluorescence using ImageJ (Potapova et al., 2011). Briefly, a region was drawn around the apical membrane region for CFTR immunofluorescence (that excluded the subapical staining). The fluorescence intensity within a selected region was then calculated. On the same slide, a measurement of an area without fluorescent objects was used as the background subtraction. To calculate the corrected fluorescence, the area of the selected tissue was multiplied by the background intensity, which was then subtracted from the intensity of the selected region. Corrected fluorescence values were expressed relative to the control tissues, which were given a value of 1.0.

Whole-intestine, cytoplasm and cell membrane isolation

Sections of the posterior intestine were mounted onto Ussing chambers, as described above for measuring I_{SC}, and treated with RGN and H-89. The physiological data were used to correlate changes in CFTR trafficking to I_{SC} and G_{TE}. Samples were prepared for western blot analysis following a modified protocol used previously in fish (Tresguerres et al., 2007). Briefly, tissues were snap frozen in liquid nitrogen and stored at −80°C. In order to achieve sufficient protein yield, tissues from each treatment were pooled in groups of three and were pulverized in a porcelain grinder and weighed, after which ice-cold homogenization buffer [250 mmol l^{-1} sucrose, 1 mmol l^{-1} EDTA, 1× HALT Protease Inhibitor Cocktail (Thermo Fisher Scientific) and 30 mmol l^{-1} Tris pH 7.4] was added in a 1:10 w/v ratio. Samples were sonicated on ice for three 10-s pulses, and centrifuged (3000 ***g***, 10 min at 4°C). The supernatant was collected; some was stored as the whole-intestine sample and the rest was centrifuged once more (20,800 ***g***, 30 min at 4°C). The supernatant was collected (the cytoplasmic fraction) and the pellet re-suspended in homogenization buffer (the membrane fraction). Following this, protein concentration was determined via the bicinchonic acid method (Thermo Fisher Scientific), according to the manufacturer's instructions.

Western blot analysis

Samples were prepared in Laemmli sample buffer (Bio-Rad, Hercules, CA, USA) at a concentration of 0.5–1.0 μg ml^{-1} for western blot analysis. Proteins were separated on 4–15% SDS-PAGE gels (Bio-Rad) at 200 V and transferred to polyvinylidene fluoride (PVDF) membranes via wet transfer for 60 min at 90 V. The PVDF membrane was then blocked using Pierce™ Protein-Free (PBS) Blocking Buffer (Thermo Fisher Scientific) for 1 h and then incubated at 5°C overnight in primary mouse CFTR antibody (see 'Intestinal sac preparations and immunohistochemistry', above) or with primary polyclonal rabbit Na^+/K^+-ATPase [NKA; Na^+/K^+-ATPase-α Antibody (H-300), cat. no. SC-28800, Santa Cruz Biotechnology, Dallas, TX, USA] to confirm the purity of each isolated fraction (membrane, cytoplasm and whole-intestine

Journal of Experimental Biology (2018) 221, jeb173948. doi:10.1242/jeb.173948

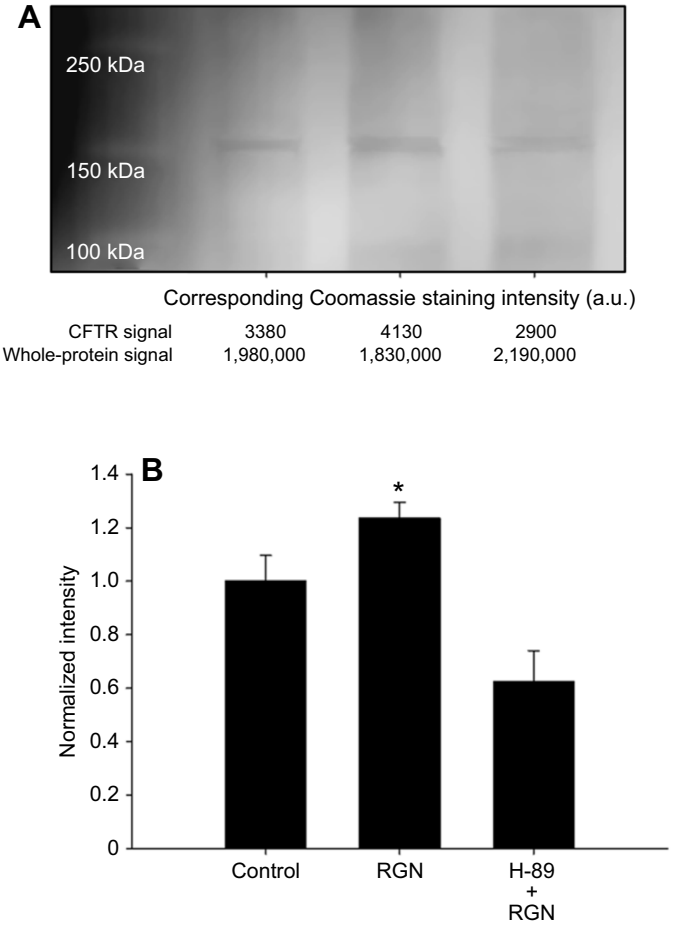

Fig. 4. RGN-stimulated CFTR translocation. (A) A representative western blot demonstrating differences in banding intensity [with representative Coomassie staining signals in arbitrary units (a.u.)] in isolated plasma membrane fragments of the posterior intestine of the Gulf toadfish. (B) Whole intestinal segments were placed in Ussing chambers and treated with a vehicle (control), RGN and RGN+H-89 (a PKA inhibitor) on the mucosal side. Quantification of membrane-present CFTR banding intensity is shown relative to control. RGN (0.1 μmol l^{-1}, dissolved in H_2O) treatment increases trafficking of CFTR to the plasma membrane of enterocytes from the posterior intestine, but this movement is inhibited by the presence of H-89 (20 μmol l^{-1}, dissolved in DMSO, final v/v 0.1%). Values are means±s.e.m. [n=3 (9 individuals pooled into three groups)]. Significant differences were revealed by a one-way ANOVA, followed by Holm–Sidak tests (*P≤0.05).

subsamples), diluted 1:150 and 1:200, respectively, with blocking buffer containing 0.05% Tween-20 (Sigma-Aldrich). The primary antibody was then discarded and blots were washed three times using Tris-buffered saline containing 0.05% Tween-20 (TBS-T). Secondary antibody for CFTR (HRP-conjugated donkey anti-mouse IgG, Santa Cruz Biotechnology) and NKA (donkey anti-rabbit IgG-HRP, cat. no. SC-2313, Santa Cruz Biotechnology), diluted 1:1500 and 1:2000, respectively, with blocking buffer containing 0.05% Tween-20 was then added to the blots, followed by incubation at room temperature for 1 h. Finally, blots were rinsed five times with TBS-T, developed using WesternSure ECL (Li-Cor, Lincoln, NE, USA), and imaged on a C-DiGit chemiluminescent scanner (Li-Cor). CFTR band intensity (~169 kDa) was determined using Image Studio Lite (Li-Cor). The control, RGN and RGN+H-89 treatments were run concurrently on the same gel to ensure complete comparability. Upon completion of the western blotting, blots were stained with Coomassie Brilliant Blue and imaged on a personal scanner, and total protein was quantified using Image Studio Lite. Western blot results were subsequently normalized to total protein in each lane to account for variations introduced during sample loading. Protein abundance was calculated relative to the appropriate control group.

Statistical analyses

The data are presented as means±s.e.m. and were evaluated using parametric and non-parametric statistical tests, as described in the figure legends. Means were considered significantly different at P≤0.05. Control measurements for I_{SC}, TEP and HCO_3^- secretion were calculated from the final 30 min of the control fluxes and treatment values were calculated from the final 30 min of a 70 min treatment exposure. All P-values for the two-tailed Holm–Sidak tests are listed in Table 2.

RESULTS

Membrane isolation and confirmation of CFTR band

NKA bands (105 kDa) were clearly visible in the membrane fraction, less so in the whole-intestine fraction, and absent in the cytoplasmic samples (Fig. 1A). This confirmed that the membrane isolation protocol was successful, as NKA is well known to be confined to the enterocyte basolateral membrane (Loretz, 1995) and, in the Atlantic salmon (*Salmo salar*) gill, has a molecular mass of 89–94 kDa (McCormick et al., 2009). Subsequently, western blots for CFTR were conducted and confirmed the presence of a band corresponding to CFTR at slightly greater than 150 kDa in the membrane fraction (Fig. 1B), in agreement with the molecular mass of human CFTR, which varies between 142 and 168 kDa (GenBank: AAA51980.1).

Stimulation by RGN and inhibition of PKA and PKG

In isolated segments of the posterior intestine, RGN stimulation reversed the absorptive I_{SC} (from mucosa-to-serosa to serosa-to-mucosa) and increased G_{TE} (Fig. 2). The effect of RGN was not altered by the addition of a PKG inhibitor (KT5823; n=8, P=0.642) (Fig. 2).

The PKA inhibitor H-89 partially, yet significantly, inhibited the effects of RGN on the absorptive I_{SC} and G_{TE} (Fig. 3A,B). H-89 alone also decreased the absorptive I_{SC}, which was fully reversed with the addition of RGN; furthermore, H-89 significantly decreased G_{TE}, which was then increased by RGN to a value that surpassed the control (Fig. 3C,D). There was no effect on I_{SC} and G_{TE} of vehicle dosages of DMSO (in which H-89 stocks were prepared; Fig. 3E,F). (All activators and inhibitors were added to the mucosal side of the tissue.)

Translocation of CFTR to the apical membrane

Western blots for CFTR revealed that RGN stimulation of posterior intestinal tissues increased the intensity of the CFTR band in the membrane fraction, while pre-treatment with H-89 eliminated changes in band intensity (Fig. 4). In addition, immunohistochemistry showed that CFTR fluorescence increased significantly in the apical membrane of RGN-treated tissues, when compared with control (Fig. 5).

HCO_3^- secretion and TEP

RGN stimulation alone reduced HCO_3^- secretion from 0.322±0.038 to 0.260±0.020 μmol cm^{-2} h^{-1} in the posterior intestine, and this was further reduced to 0.206±0.012 μmol cm^{-2} h^{-1} after the addition of H-89 (Fig. 6A). RGN also reversed the negative TEP, but had no effect on G_{TE}; the subsequent addition of H-89 partially reversed the

Journal of Experimental Biology (2018) 221, jeb173948. doi:10.1242/jeb.173948

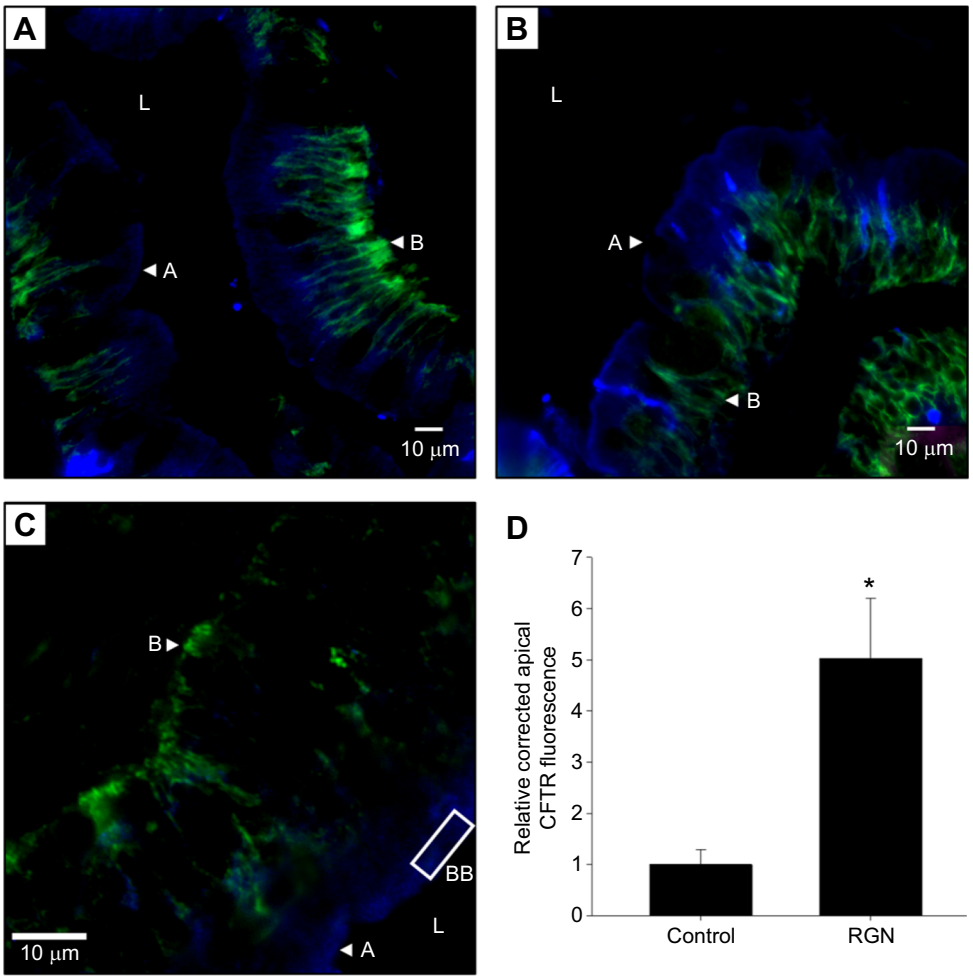

Fig. 5. Immunolocalization of CFTR. Immunohistochemsitry revealed that RGN induces increased trafficking of the CFTR to the plasma membrane of enterocytes from the posterior intestine of the Gulf toadfish. Overlaid fluorescence images of 4 μm sections from the posterior intestine of the Gulf toadfish show CFTR (blue) and NKA (green). Sections from control (A,C) and RGN-treated tissues (B) reveal different CFTR fluorescence intensity. The brush border is more clearly seen in C, demonstrating the location of the CFTR immunofluorescence in apical and sub-apical areas. Images are representative of each treatment group (n=4 each) and are shown at 40× (A,B) and 60× (C) magnification. (D) Relative corrected apical fluorescence for the CFTR, calculated from fluorescence images of the posterior intestine of Gulf toadfish. Tissues treated with RGN display greater CFTR, fluorescence relative to control tissues. Values are means±s.e.m. and significant differences were revealed by a Student's t-test (*P≤0.05). A, apical membrane; B, basolateral membrane; L, lumen; BB, brush border.

effect on TEP of RGN and decreased G_{TE} (Fig. 6B). Comparatively, H-89 alone had no effect on HCO_3^- secretion (0.284±0.012 and 0.273±0.022 μmol cm^{-2} h^{-1}, control and H-89 treatment, respectively); however, the addition of RGN did reduce HCO_3^- secretion to 0.258±0.025 μmol cm^{-2} h^{-1} (Fig. 6C). G_{TE} was reduced by H-89 alone and the negative TEP was reversed by the combination of H-89 and RGN (Fig. 6D). A Student's t-test revealed that baseline HCO_3^- secretion ($\Delta J_{HCO_3^-}$) was decreased to a greater extent by RGN alone (17.5±3.9%) than by RGN added after H-89 (9.6±3.3%) (Fig. 6A,C; P=0.018). This indicates an inhibitory effect of H-89 on RGN-induced responses.

DISCUSSION

The present study confirmed the presence of CFTR in the plasma membrane of the posterior intestine of the Gulf toadfish by western blot analysis and apical localization by immunohistochemistry. There was increased translocation of CFTR to the apical membrane after stimulation of the enterocytes with RGN that coincided with a reversal of the absorptive I_{SC}, which was suppressed by PKA inhibition. RGN stimulation also led to inhibition of HCO_3^- secretion. The downstream effects of RGN stimulation seem to be primarily mediated by PKA, rather than PKG.

The downstream effects of RGN on PKA

Guanylin, uroguanylin and RGN are endogenous activators of GC-C in vertebrates (Currie et al., 1992; Greenberg et al., 1997; Hamra et al., 1993; Yuge and Takei, 2007) and have been shown to regulate body electrolyte and fluid homeostasis by modulating the activity of various ion transporters (Arshad and Visweswariah, 2012; Forte, 1999; Forte and Hamra, 1996). In vertebrates, this occurs through elevated cGMP formation (Currie et al., 1992; Iio et al., 2005; Yuge et al., 2006), which can increase PKG activity, modulate cAMP abundance and regulate PKA activity (Arshad and Visweswariah, 2013). The results of the present study on the Gulf toadfish suggest a greater role for PKA, rather than PKG, in the downstream pathways activated by RGN. Indeed, inhibition of PKA (by H-89) significantly reversed the effect of RGN on the absorptive I_{SC} and TEP, while inhibition of PKG did not. However, the inhibitory effect of PKA was partial and might be due to the fact that (i) PKA is involved in more than one signaling pathway, (ii) H-89 will target all PKA molecules within a cell and not just those involved in guanylin-peptide signaling and/or (iii) numerous cellular pathways are involved in the response, not just those regulated by PKA. Perhaps pre-treatment with H-89 prior to RGN addition results in the modulation of multiple intracellular pathways that relate to osmoregulation and cAMP/PKA. Consequently, the effects of H-89 might not be clear and could be masked once RGN is added, whereas this might not be the case when H-89 is added after RGN treatment.

PKA inhibition alone (in the absence of RGN) also decreased the absorptive I_{SC} and TEP, a result that is not surprising, given the ubiquitous involvement of cAMP and PKA in cellular processes, including ion transport mechanisms. For example, cAMP/PKA has been implicated in NKCC2 stimulation in the Gulf toadfish and sea

Journal of Experimental Biology (2018) 221, jeb173948. doi:10.1242/jeb.173948

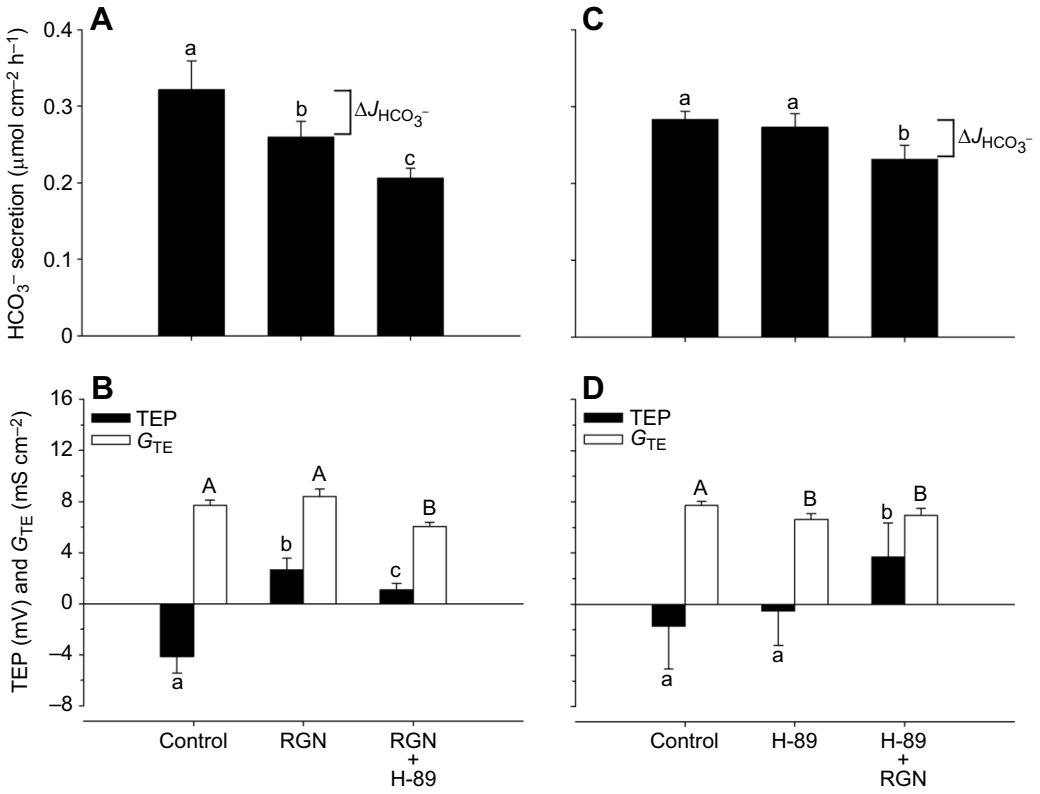

Fig. 6. Modulation of HCO_3^- secretion. HCO_3^- secretion (A,C), and transepithelial potential (TEP) and G_{TE} (B,D) displayed by the posterior intestine of Gulf toadfish. Control values were taken from the final 30 min of the control flux. RGN or H-89 (a PKA inhibitor) was then added, and its effects were measured from the final 30 min of a 70 min treatment flux. Finally, H-89 or RGN was added to the first treatment, and their overall effects were measured from the final 30 min of a 70 min treatment flux (t_{total}=170 min). Values are means±s.e.m. Significant differences were revealed by one-way, repeated-measures ANOVA, followed by Holm–Sidak tests ($^{a,b,c}P \leq 0.05$). Positive and negative TEP values indicate net anion secretion and absorption, respectively. RGN (0.1 μmol l^{-1}, dissolved in H_2O) and H-89 (20 μmol l^{-1}, dissolved in DMSO, final v/v 0.1%) were added to the mucosal half-chamber of the Ussing apparatus.

bream (*Sparus aurata*) intestine (Carvalho et al., 2012; Tresguerres et al., 2010) and PKA has been shown to phosphorylate NKCC2 in the thick ascending limb of rats (Ares et al., 2011); both of these mechanisms stimulate ion absorption. Accordingly, their inhibition would reduce ion absorption, similar to what is observed in the posterior intestine of Gulf toadfish.

Although it is beyond the scope of the present study, RGN activation of GC-C (which has intrinsic GC activity) increases intracellular cGMP formation in fish (Yuge et al., 2006) and mammals (Forte et al., 1993), and the effect of cGMP in this signaling pathway seems to be mediated more by PKA than by PKG. Indeed, in T_{84} cells (which originate from human colon carcinomas), stimulation of GC-C by either STa (the heat-stable *Escherichia coli* enterotoxin that also activates GC-C) or guanylin elevates cGMP formation, leading to changes in cellular physiology, but these effects are negated by PKA inhibition (Chao et al., 1994). Previous research suggests that there are two possible pathways by which increased cGMP formation is primarily mediated downstream by PKA. The first is indirect activation by inhibition of phosphodiesterase 3 (which cleaves cAMP to its inactive, linear form, AMP), which allows the accumulation of cAMP (Arshad, and Visweswariah, 2013). The second is a putative pathway by which cGMP directly activates PKA, which is suggested to occur in the Japanese tree frog (*Hyla japonica*), after stimulation of urinary bladder cells by atrial natriuretic peptide (Yamada et al., 2006, 2007). Whatever the pathway might be, prior research on the winter flounder demonstrates that PKA plays a prominent role in intestinal physiology (using VIP and cAMP, both of which are upstream regulators of PKA) by inhibiting ion transport and producing secretory currents (O'Grady, 1989; O'Grady et al., 1988; Rao et al., 1984). Accordingly, PKA is a possible candidate for mediating the intracellular effects of the guanylin peptides in seawater teleosts.

RGN stimulation leads to increased apical CFTR activation and trafficking

This is the first study to reveal membrane trafficking of CFTR in the Gulf toadfish that is stimulated by RGN. Although it merits further study, RGN can lead to CFTR translocation (present study) or modulate CFTR ion transport (Ruhr et al., 2014). Both of these mechanisms are supported by mammalian and fish studies. In the villi of the rat jejunum, STa and cAMP induce CFTR translocation to the apical membrane and their effects are decreased by PKA inhibition (Golin-Bisello et al., 2005). Likewise, the regulation of CFTR by cAMP/PKA pathways has also been documented in several fish species. For example, in the opercular epithelium of killifish and in the rectal gland of spiny dogfish shark (*Squalus acanthias*), cAMP/PKA has been implicated in CFTR activation (de Jonge et al., 2014; Marshall et al., 2005). Correspondingly, the present study also shows that RGN stimulation increases CFTR translocation to the apical membrane and that the translocation is suppressed by PKA inhibition, similar to findings in the rat jejunum (Golin-Bisello et al., 2005). Additionally, stimulation of Gulf toadfish posterior intestinal tissues by RGN leads to Cl^- efflux (Ruhr et al., 2015, 2016) and is mediated by CFTR (Ruhr et al., 2014). Moreover, because of the short duration of the experiments,

Journal of Experimental Biology (2018) 221, jeb173948. doi:10.1242/jeb.173948

in which tissues were treated with RGN for 70–140 min, it is unlikely that the changes in membrane-localized CFTR observed during RGN treatment could be due to changes in protein expression. Indeed, in a previous study on the Gulf toadfish intestine, exposure to 60 ppt seawater significantly increased CFTR mRNA expression after 24 h, but not before 12 h (Ruhr et al., 2015). Although the present study does not definitively show CFTR in the apical membrane of the Gulf toadfish intestine, we have previously shown that blocking CFTR with an inhibitor prevents the reversal of the absorptive I_{SC} by RGN when applied to the apical membrane (Ruhr et al., 2014), while its basolateral application has no effect (I.M.R., personal observations). Accordingly, the combined evidence using CFTR inhibition (Ruhr et al., 2014), apical immunofluorescence in the intestine [present and previous studies (Ruhr et al., 2014)] and western blots on membrane fragments (present study) is compelling in proposing an apical localization of CFTR in the Gulf toadfish intestine. Moreover, there exists the possibility of more than one CFTR isoform being expressed in the Gulf toadfish intestine, as occurs in the Japanese eel (Wong et al., 2016), which could be regulated differently by RGN. Taken together, the current and previous (Ruhr et al., 2014) studies on the Gulf toadfish posterior intestine support the idea that RGN both activates membrane-present CFTR and increases CFTR trafficking to the apical membrane. On a final note, as with many biological mechanisms, CFTR trafficking might be regulated by proteins other than cAMP/PKA. An example relevant to the present study is serum and glucocorticoid-regulated kinase 1 (SGK1), which is a well-known osmotic stress transcription factor found in many vertebrates, including the fish intestine (Wong et al., 2014). SGK1 protein abundance is elevated in the intestine of killifish upon transfer to seawater from freshwater, an increase that is absent following morpholino gene knockdown (Notch et al., 2011). When SGK1 protein synthesis is suppressed in this manner, there is also a corresponding suppression of CFTR insertion into the plasma membrane of the intestine during seawater exposure (Notch et al., 2011). These results are similar to observations in the present study, prompting the question: what other possible proteins, enzymes or intracellular pathways does guanylin-peptide stimulation modulate? Undoubtedly, more research on this topic must be carried out.

Does RGN affect apical HCO_3^- transport via PKA?

In the present and previous studies, posterior intestinal tissues from Gulf toadfish displayed decreased HCO_3^- secretion when exposed to RGN (Ruhr et al., 2014, 2015, 2016). However, the mechanism by which this occurs is unknown, although it has been suggested that it involves apical HCO_3^-/Cl^- exchangers, such as SLC26a6 (Ruhr et al., 2016), which is the major HCO_3^--secretory transporter in the Gulf toadfish intestine (Grosell, 2006). The present study looked at the possible effect of RGN on the relationship between PKA and HCO_3^- secretion. In the presence of RGN alone, the posterior intestine of Gulf toadfish displayed decreased HCO_3^- secretion. However, when tissues were pre-treated with the PKA inhibitor H-89 prior to RGN addition, the effect of RGN on HCO_3^- secretion was almost halved compared with when RGN was added alone (17.5±3.9% decrease with RGN alone versus 9.6±3.3% with RGN+H-89). These data suggest that decreases in HCO_3^- secretion might be partially mediated by elevated PKA activity, as a result of RGN stimulation. This mechanism is similar to what has been proposed in mammalian models, in which the secondary messengers cAMP and PKC inhibit SLC26 transporters by internalization (Kato and Romero, 2011). Nevertheless, it is still unknown which HCO_3^- transporter is affected by the downstream effects of RGN, as there are additional bicarbonate transporters (SLC26a3 and SLC4a2), other than SLC26a6, present in the apical membrane (Grosell, 2011). Despite this gap in our knowledge, there exist further comparable mechanisms for decreasing HCO_3^- secretion in other animals. Indeed, in the sea bream, stimulation of putative soluble adenylyl cyclase (sAC), which produces cAMP in intestinal tissues, results in increased HCO_3^- secretion (Carvalho et al., 2012), possibly mediated by PKA. For mammals, there is a larger body of work that corroborates what has been seen in fish [see reviews or studies on the pancreas (Ishiguro et al., 2012), exocrine glands (Hong et al., 2014) and intestine (Ko et al., 2002)]. In rat renal proximal tubular epithelial cells, both a cAMP analog and forskolin increase HCO_3^- secretion, which is believed to elevate the exchange activity of SLC26a6; these stimulatory effects are inhibited by PKA inhibition via H-89 (Simão et al., 2008). Conversely, to our knowledge, only one study has demonstrated the direct effects of phosphorylation on SLC26a6 exchange activity (Alvarez et al., 2005). This study revealed that PKC phosphorylates human SLC26a6, leading to the disruption of a metabolon between SLC26a6 and carbonic anhydrase II, which decreases HCO_3^- secretion (Alvarez et al., 2005). However, that study investigated the role of PKC, as opposed to the present study, which looked at the effects of PKG and PKA on HCO_3^- secretion. Overall, the previous studies and our present study support the hypothesis that RGN decreases HCO_3^- secretion in Gulf toadfish intestine,

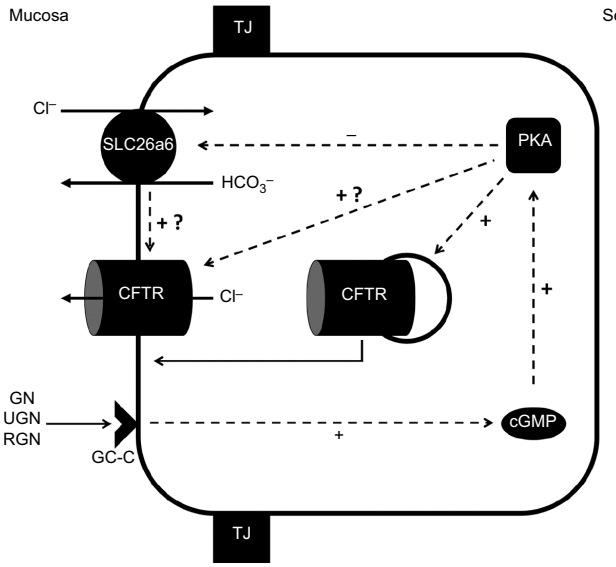

Fig. 7. Intracellular effects of guanylin peptides. Simplified proposed effects of the guanylin peptides in the enterocytes of the posterior intestine of Gulf toadfish. Guanylin (GN), uroguanylin (UGN) and renoguanylin (RGN) bind to a guanylyl cyclase-C (GC-C) receptor on the apical membrane of an enterocyte. The stimulation of GC-C, which has intrinsic GC activity, leads to enhanced formation of cyclic guanosine monophosphate (cGMP), the downstream effects of which appear to stimulate protein kinase A (PKA) activity. Once activated, PKA (i) reduces HCO_3^- secretion, possibly by altering anion exchange activity (in the case of the Gulf toadfish, this would occur primarily by inhibiting SLC26a6 transport); this also triggers (ii) the opening of membrane-present CFTR Cl^- channels (either through direct phosphorylation by PKA or as a result of interactions with SLC26 transporters) and (iii) the insertion of CFTR into the plasma membrane. From previous studies on teleost fish, the combined effects of GC-C stimulation result in the reversal of ion flux, from net ion absorption (mucosa-to-serosa) to net ion secretion (serosa-to-mucosa), which leads to inhibited water absorption (Ruhr et al., 2014, 2015, 2016). TJ, tight junction; +, stimulatory effects; –, inhibitory effects.

possibly by stimulating PKA activity, but the exact intracellular mechanisms by which they occur are still unclear.

Conclusions

The present study revealed that RGN stimulation of the posterior intestine appears to elevate PKA activity (Fig. 7). Upon binding to its receptor, RGN could regulate HCO_3^- and Cl^- transport by modifying potential interactions between SLC26 transporters and CFTR in the Gulf toadfish, as described in the rat intestine. Briefly, the rat intestinal model proposes that SLC26 transporters and CFTR form complexes that interact with one another through binding proteins, and that SLC26 transporters regulate CFTR activity (Ko et al., 2004). However, there are two main differences between the rat and Gulf toadfish, with respect to HCO_3^- transport and the direction of Cl^- movement through CFTR. In the rat intestine, stimulation of HCO_3^- secretion by SLC26 transporters also stimulates Cl^- absorption by CFTR (Ko et al., 2004); conversely, in the Gulf toadfish intestine, inhibition of HCO_3^- secretion correlates with stimulated Cl^- secretion by CFTR in the Gulf toadfish (Ruhr et al., 2014, 2015). Alternatively, the effect of RGN stimulation could be mediated by PKA acting within intracellular microdomains (co-assemblages of proteins), affecting local signaling. Although speculative in the present context (and requiring further study), the presence of microdomains would be advantageous, as they allow endogenous stimulators (e.g. hormones) to activate specific intracellular pathways that are targeted by cAMP and PKA, rather than all pathways involving these molecules (Cooper, 2003; Zaccolo et al., 2006).

Overall, the present study demonstrates that PKA potentially mediates the downstream effects of RGN in the Gulf toadfish intestine by decreasing HCO_3^- secretion, inhibiting absorptive ion transport, and increasing CFTR trafficking to the apical membrane. Although it is tempting to speculate that this response is associated with GC-Cs in Gulf toadfish intestinal tissues, RGN could also be operating via other receptors evolved to mediate RGN or other guanylin-like peptides. Regardless of which receptor mediates the guanylin-peptide response, previous research on the seawater teleost intestine shows that guanylin-peptide stimulation leads to a reversal of net ion flux (from absorption to secretion) and decreased HCO_3^- secretion, with the overall effect of inhibited (or reversed) water absorption by the intestine (Ando and Takei, 2015; Ando et al., 2014; Ruhr et al., 2014, 2015, 2016; Yuge and Takei, 2007). These effects appear to occur by inhibited NKCC2 transport, activation of CFTR and Cl^- secretion, and inhibited HCO_3^-/Cl^- exchange activity (Ruhr et al., 2014, 2016). However, the present study reveals that these changes to ion flux might be a function of CFTR insertion into the apical membrane, which is mediated, in part, by PKA, as well as the direct effects on membrane-present CFTR function. Despite what is known about the guanylin peptides in seawater teleosts, their functional importance to whole-animal physiology is still unclear and merits further study.

Acknowledgements

We thank Drs M. Danielle McDonald and Michael C. Schmale from the Rosenstiel School of Marine and Atmospheric Science at the University of Miami for the generous use of their equipment.

Competing interests

The authors declare no competing or financial interests.

Author contributions

Conceptualization: I.M.R., M.G.; Methodology: I.M.R., K.L.S., Y.T., M.G.; Validation: I.M.R., M.G.; Formal analysis: I.M.R., K.L.S., M.G.; Investigation: I.M.R., M.G.; Resources: M.G.; Data curation: I.M.R.; Writing - original draft: I.M.R.; Writing - review & editing: I.M.R., K.L.S., Y.T., M.G.; Visualization: I.M.R.; Supervision: M.G.; Project administration: M.G.; Funding acquisition: M.G.

Funding

M.G. is Maytag Professor of Ichthyology and is supported by the National Science Foundation (IOS 1146695).

References

Alvarez, B. V., Vilas, G. L. and Casey, J. R. (2005). Metabolon disruption: a mechanism that regulates bicarbonate transport. *EMBO J.* **24**, 2499-2511.

Ando, M. and Takei, Y. (2015). Guanylin activates Cl^- secretion into the lumen of seawater eel intestine via apical Cl^- channel under simulated in vivo conditions. *Am. J. Physiol. Regul. Integr. Comp. Physiol.* **308**, R400-R410.

Ando, M., Wong, M. K. S. and Takei, Y. (2014). Mechanisms of guanylin action on water and ion absorption at different regions of seawater eel intestine. *Am. J. Physiol. Regul. Integr. Comp. Physiol.* **307**, R653-R663.

Ares, G. R., Caceres, P. S. and Ortiz, P. A. (2011). Molecular regulation of NKCC2 in the thick ascending limb. *Am. J. Physiol. Renal. Physiol.* **301**, F1143-F1159.

Arshad, N. and Visweswariah, S. S. (2012). The multiple and enigmatic roles of guanylyl cyclase C in intestinal homeostasis. *FEBS Lett.* **586**, 2835-2840.

Arshad, N. and Visweswariah, S. S. (2013). Cyclic nucleotide signaling in intestinal epithelia: getting to the gut of the matter. *Wiley Interdiscip. Rev. Syst. Biol. Med.* **5**, 409-424.

Carvalho, E. S. M., Gregório, S. F., Power, D. M., Canário, A. V. M. and Fuentes, J. (2012). Water absorption and bicarbonate secretion in the intestine of the sea bream are regulated by transmembrane and soluble adenylyl cyclase stimulation. *J. Comp. Physiol. B* **182**, 1069-1080.

Chao, A. C., de Sauvage, F. J., Dong, Y. J., Wagner, J. A., Goeddel, D. V. and Gardner, P. (1994). Activation of intestinal CFTR Cl^- channel by heat-stable enterotoxin and guanylin via cAMP-dependent protein kinase. *EMBO J.* **13**, 1065-1072.

Cooper, D. M. F. (2003). Regulation and organization of adenylyl cyclases and cAMP. *Biochem. J.* **375**, 517-529.

Currie, M. G., Fok, K. F., Kato, J., Moore, R. J., Hamra, F. K., Duffin, K. L. and Smith, C. E. (1992). Guanylin: an endogenous activator of intestinal guanylate cyclase. *Proc. Natl. Acad. Sci. USA* **89**, 947-951.

de Jonge, H. R., Tilly, B. C., Hogema, B. M., Pfau, D. J., Kelley, C. A., Kelley, M. H., Melita, A. M., Morris, M. T., Viola, R. M. and Forrest, J. N. (2014). cGMP inhibition of type 3 phosphodiesterase is the major mechanism by which C-type natriuretic peptide activates CFTR in the shark rectal gland. *Am. J. Physiol. Cell Physiol.* **306**, C343-C353.

Evans, D. H., Piermarini, P. M. and Choe, K. P. (2005). The multifunctional fish gill: dominant site of gas exchange, osmoregulation, acid-base regulation, and excretion of nitrogenous waste. *Physiol. Rev.* **85**, 97-177.

Forte, L. R. (1999). Guanylin regulatory peptides: structures, biological activities mediated by cyclic GMP and pathobiology. *Regul. Pept.* **81**, 25-39.

Forte, L. R. and Hamra, F. K. (1996). Guanylin and uroguanylin: intestinal peptide hormones that regulate epithelial transport. *News Physiol. Sci.* **11**, 17-24.

Forte, L. R., Eber, S. L., Turner, J. T., Freeman, R. H., Fok, K. F. and Currie, M. G. (1993). Guanylin stimulation of Cl^- secretion in human intestinal T84 cells via cyclic guanosine monophosphate. *J. Clin. Invest.* **91**, 2423-2428.

Goode, G. B., and Bean, T. H. (1880). Catalogue of a collection of fishes obtained in the Gulf of Mexico, by Dr. J. W. Velie, with descriptions of seven new species. *Proc. US Natl. Mus.* **2**, 333-345.

Golin-Bisello, F., Bradbury, N. and Ameen, N. (2005). STa and cGMP stimulate CFTR translocation to the surface of villus enterocytes in rat jejunum and is regulated by protein kinase G. *Am. J. Physiol. Cell Physiol.* **289**, C708-C716.

Greenberg, R. N., Hill, M., Crytzer, J., Krause, W. J., Eber, S. L., Hamra, F. K. and Forte, L. R. (1997). Comparison of effects of uroguanylin, guanylin, and *Escherichia coli* heat-stable enterotoxin STa in mouse intestine and kidney: evidence that uroguanylin is an intestinal natriuretic hormone. *J. Inv. Med.* **45**, 276-283.

Grosell, M. (2006). Intestinal anion exchange in marine fish osmoregulation. *J. Exp. Biol.* **209**, 2813-2827.

Grosell, M. (2011). Intestinal anion exchange in marine teleosts is involved in osmoregulation and contributes to the oceanic inorganic carbon cycle. *Acta Physiol. (Oxf.)* **202**, 421-434.

Grosell, M. and Genz, J. (2006). Ouabain-sensitive bicarbonate secretion and acid absorption by the marine teleost fish intestine play a role in osmoregulation. *Am. J. Physiol. Regul. Integr. Comp. Physiol.* **291**, R1145-R1156.

Grosell, M., Genz, J., Taylor, J. R., Perry, S. F. and Gilmour, K. M. (2009a). The involvement of H^+-ATPase and carbonic anhydrase in intestinal HCO_3^- secretion in seawater-acclimated rainbow trout. *J. Exp. Biol.* **212**, 1940-1948.

Grosell, M., Mager, E. M., Williams, C. and Taylor, J. R. (2009b). High rates of HCO_3^- secretion and Cl^- absorption against adverse gradients in the marine teleost intestine: the involvement of an electrogenic anion exchanger and H^+-pump metabolon? *J. Exp. Biol.* **212**, 1684-1696.

Hamra, F. K., Forte, L. R., Eber, S. L., Pidhorodeckyj, N. V., Krause, W. J., Freeman, R. H., Chin, D. T., Tompkins, J. A., Fok, K. F. and Smith, C. E. (1993).

Uroguanylin: structure and activity of a second endogenous peptide that stimulates intestinal guanylate cyclase. *Proc. Natl. Acad. Sci. USA* **90**, 10464-10468.

Hong, J. H., Park, S., Shcheynikov, N. and Muallem, S. (2014). Mechanism and synergism in epithelial fluid and electrolyte secretion. *Pflügers Arch.* **466**, 1487-1499.

Iio, K., Nakauchi, M., Yamagami, S., Tsutsumi, M., Hori, H., Naruse, K., Mitani, H., Shima, A. and Suzuki, N. (2005). A novel membrane guanylyl cyclase expressed in medaka (*Oryzias latipes*) intestine. *Comp. Biochem. Physiol. B Biochem. Mol. Biol.* **140**, 569-578.

Ishiguro, H., Yamamoto, A., Nakakuki, M., Yi, L., Ishiguro, M., Yamaguchi, M., Kondo, S. and Mochimaru, Y. (2012). Physiology and pathophysiology of bicarbonate secretion by pancreatic duct epithelium. *Nagoya J. Med. Sci.* **74**, 1-18.

Kato, A. and Romero, M. F. (2011). Regulation of electroneutral NaCl absorption by the small intestine. *Annu. Rev. Physiol.* **73**, 261.

Ko, S. B. H., Shcheynikov, N., Choi, J. Y., Luo, X., Ishibashi, K., Thomas, P. J., Kim, J. Y., Kim, K. H., Lee, M. G., Naruse, S. et al. (2002). A molecular mechanism for aberrant CFTR-dependent HCO_3^- transport in cystic fibrosis. *EMBO J.* **21**, 5662-5672.

Ko, S. B. H., Zeng, W., Dorwart, M. R., Luo, X., Kim, K. H., Millen, L., Goto, H., Naruse, S., Soyombo, A., Thomas, P. J. et al. (2004). Gating of CFTR by the STAS domain of SLC26 transporters. *Nat. Cell Biol.* **6**, 343-350.

Kuhn, M., Adermann, K., Jähne, J., Forssmann, W. G. and Rechkemmer, G. (1994). Segmental differences in the effects of guanylin and *Escherichia coli* heat-stable enterotoxin on Cl^- secretion in human gut. *J. Physiol.* **479**, 433-440.

Loretz, C. A. (1995). 2 Electrophysiology of ion transport in teleost intestinal cells. *Fish Physiol.* **14**, 25-56.

Marshall, W. S., Howard, J. A., Cozzi, R. R. and Lynch, E. M. (2002). NaCl and fluid secretion by the intestine of the teleost *Fundulus heteroclitus*: involvement of CFTR. *J. Exp. Biol.* **205**, 745-758.

Marshall, W. S., Ossum, C. G. and Hoffmann, E. K. (2005). Hypotonic shock mediation by p38 MAPK, JNK, PKC, FAK, OSR1 and SPAK in osmosensing chloride secreting cells of killifish opercular epithelium. *J. Exp. Biol.* **208**, 1063-1077.

McCormick, S. D., Regish, A. M. and Christensen, A. K. (2009). Distinct freshwater and seawater isoforms of Na^+/K^+-ATPase in gill chloride cells of Atlantic salmon. *J. Exp. Biol.* **212**, 3994-4001.

Notch, E. G., Shaw, J. R., Coutermarsh, B. A., Dzioba, M. and Stanton, B. A. (2011). Morpholino gene knockdown in adult *Fundulus heteroclitus*: role of SGK1 in seawater acclimation. *PLoS ONE* **6**, e29462.

O'Grady, S. M. (1989). Cyclic nucleotide-mediated effects of ANF and VIP on flounder intestinal ion transport. *Am. J. Physiol. Regul. Integr. Comp. Physiol.* **256**, C142-C146.

O'Grady, S. M. and Wolters, P. J. (1990). Evidence for chloride secretion in the intestine of the winter flounder. *Am. J. Physiol. Regul. Integr. Comp. Physiol.* **258**, C243-C247.

O'Grady, S. M., Field, M., Nash, N. T. and Rao, M. C. (1985). Atrial natriuretic factor inhibits Na-K-Cl cotransport in teleost intestine. *Am. J. Physiol. Regul. Integr. Comp. Physiol.* **249**, C531-C534.

O'Grady, S. M., DeJonge, H. R., Vaandrager, A. B. and Field, M. (1988). Cyclic nucleotide-dependent protein kinase inhibition by H-8: effects on ion transport. *Am. J. Physiol. Regul. Integr. Comp. Physiol.* **254**, C115-C121.

Potapova, T. A., Sivakumar, S., Flynn, J. N., Li, R. and Gorbsky, G. J. (2011). Mitotic progression becomes irreversible in prometaphase and collapses when Wee1 and Cdc25 are inhibited. *Mol. Biol. Cell* **22**, 1191-1206.

Rao, M. C. and Nash, N. T. (1988). 8-BrcAMP does not affect Na-K-2Cl cotransport in winter flounder intestine. *Am. J. Physiol. Cell Physiol.* **255**, C246-C251.

Rao, M. C., Nash, N. T. and Field, M. (1984). Differing effects of cGMP and cAMP on ion transport across flounder intestine. *Am. J. Physiol. Regul. Integr. Comp. Physiol.* **246**, C167-C171.

Ruhr, I. M., Bodinier, C., Mager, E. M., Esbaugh, A. J., Williams, C., Takei, Y. and Grosell, M. (2014). Guanylin peptides regulate electrolyte and fluid transport in the Gulf toadfish (*Opsanus beta*) posterior intestine. *Am. J. Physiol. Regul. Integr. Comp. Physiol.* **307**, R1167-R1179.

Ruhr, I. M., Mager, E. M., Takei, Y. and Grosell, M. (2015). The differential role of renoguanylin in osmoregulation and apical Cl^-/HCO_3^- exchange activity in the posterior intestine of the Gulf toadfish (*Opsanus beta*). *Am. J. Physiol. Regul. Integr. Comp. Physiol.* **309**, R399-R409.

Ruhr, I. M., Takei, Y. and Grosell, M. (2016). The role of the rectum in osmoregulation and the potential effect of renoguanylin on SLC26a6 transport activity in the Gulf toadfish (*Opsanus beta*). *Am. J. Physiol. Regul. Integr. Comp. Physiol.* **311**, R179-R191.

Schindelin, J., Arganda-Carreras, I., Frise, E., Kaynig, V., Longair, M., Pietzsch, T., Preibisch, S., Rueden, C., Saalfeld, S., Schmid, B. et al. (2012). Fiji: an open-source platform for biological-image analysis. *Nat. Methods* **9**, 676-682.

Schulz, S., Green, C. K., Yuen, P. S. T. and Garbers, D. L. (1990). Guanylyl cyclase is a heat-stable enterotoxin receptor. *Cell* **63**, 941-948.

Schulze, K. S. (2015). The imaging and modelling of the physical processes involved in digestion and absorption. *Acta Physiol. (Oxf.)* **213**, 394-405.

Simão, S., Pedrosa, R., Hopfer, U., Mount, D. B., Jose, P. A. and Soares-da-Silva, P. (2008). Short-term regulation of the Cl^-/HCO_3^- exchanger in immortalized SHR proximal tubular epithelial cells. *Biochem. Pharmacol.* **75**, 2224-2233.

Skadhauge, E. (1969). The mechanism of salt and water absorption in the intestine of the eel (*Anguilla anguilla*) adapted to waters of various salinities. *J. Physiol.* **204**, 135-158.

Skadhauge, E. (1974). Coupling of transmural flows of NaCl and water in the intestine of the eel (*Anguilla anguilla*). *J. Exp. Biol.* **60**, 535-546.

Tresguerres, M., Parks, S. K., Wood, C. M. and Goss, G. G. (2007). V-H^+-ATPase translocation during blood alkalosis in dogfish gills: interaction with carbonic anhydrase and involvement in the postfeeding alkaline tide. *Am. J. Physiol. Regul. Integr. Comp. Physiol.* **292**, R2012-R2019.

Tresguerres, M., Levin, L. R., Buck, J. and Grosell, M. (2010). Modulation of NaCl absorption by $[HCO_3^-]$ in the marine teleost intestine is mediated by soluble adenylyl cyclase. *Am. J. Physiol. Regul. Integr. Comp. Physiol.* **299**, R62-R71.

Weber, W.-M., Cuppens, H., Cassiman, J.-J., Clauss, W. and Van Driessche, W. (1999). Capacitance measurements reveal different pathways for the activation of CFTR. *Pflugers Arch.* **438**, 561-569.

Wilson, R. W., Wilson, J. M. and Grosell, M. (2002). Intestinal bicarbonate secretion by marine teleost fish – why and how? *Biochim. Biophys. Acta Biomemb.* **1566**, 182-193.

Wong, M. K.-S., Ozaki, H., Suzuki, Y., Iwasaki, W. and Takei, Y. (2014). Discovery of osmotic sensitive transcription factors in fish intestine via a transcriptomic approach. *BMC Genomics* **15**, 1134.

Wong, M. K.-S., Pipil, S., Kato, A. and Takei, Y. (2016). Duplicated CFTR isoforms in eels diverged in regulatory structures and osmoregulatory functions. *Comp. Biochem. Physiol. A Mol. Integr. Physiol.* **199**, 130-141.

Yamada, T., Matsuda, K. and Uchiyama, M. (2006). Atrial natriuretic peptide and cGMP activate sodium transport through PKA-dependent pathway in the urinary bladder of the Japanese tree frog. *J. Comp. Physiol. B* **176**, 203-212.

Yamada, T., Matsuda, K. and Uchiyama, M. (2007). Frog ANP increases the amiloride-sensitive Na^+ channel activity in urinary bladder cells of Japanese tree frog, Hyla japonica. *Gen. Comp. Endocrinol.* **152**, 286-288.

Yuge, S. and Takei, Y. (2007). Regulation of ion transport in eel intestine by the homologous guanylin family of peptides. *Zoolog. Sci.* **24**, 1222-1230.

Yuge, S., Yamagami, S., Inoue, K., Suzuki, N. and Takei, Y. (2006). Identification of two functional guanylin receptors in eel: multiple hormone-receptor system for osmoregulation in fish intestine and kidney. *Gen. Comp. Endocrinol.* **149**, 10-20.

Zaccolo, M., Di Benedetto, G., Lissandron, V., Mancuso, L., Terrin, A. and Zamparo, I. (2006). Restricted diffusion of a freely diffusible second messenger: mechanisms underlying compartmentalized cAMP signalling. *Biochem. Soc. Trans.* **34**, 495-497.